MOLECULAR AND CELLULAR BIOLOGY, June 2003, p. 3884–3896 Vol. 23, No. 11
0270-7306/03/$08.00+0 DOI: 10.1128/MCB.23.11.3884–3896.2003

Two Distinct Phosphorylation Pathways Have Additive Effects on Abl Family Kinase Activation

Keith Q. Tanis,[1] Darren Veach,[2] Henry S. Duewel,[3] William G. Bornmann,[2] and Anthony J. Koleske[1]*

Department of Molecular Biophysics and Biochemistry, Yale University, New Haven, Connecticut 06520[1]; Organic Synthesis Core Facility, Sloan-Kettering Institute for Cancer Research, New York, New York 10021[2]; and MDS Proteomics, Toronto, Ontario M9W 7H4, Canada[3]

Received 7 November 2002/Returned for modification 17 December 2002/Accepted 4 March 2003

The activities of the related Abl and Arg nonreceptor tyrosine kinases are kept under tight control in cells, but exposure to several different stimuli results in a two- to fivefold stimulation of kinase activity. Following the breakdown of inhibitory intramolecular interactions, Abl activation requires phosphorylation on several tyrosine residues, including a tyrosine in its activation loop. These activating phosphorylations have been proposed to occur either through autophosphorylation by Abl in *trans* or through phosphorylation of Abl by the Src nonreceptor tyrosine kinase. We show here that these two pathways mediate phosphorylation at distinct sites in Abl and Arg and have additive effects on Abl and Arg kinase activation. Abl and Arg autophosphorylate at several sites outside the activation loop, leading to 5.2- and 6.2-fold increases in kinase activity, respectively. We also find that the Src family kinase Hck phosphorylates the Abl and Arg activation loops, leading to an additional twofold stimulation of kinase activity. The autoactivation pathway may allow Abl family kinases to integrate or amplify cues relayed by Src family kinases from cell surface receptors.

Protein kinases transmit information by phosphorylating specific substrates in response to discrete stimuli. The two vertebrate Abl family nonreceptor tyrosine kinases, Abl and Arg, have been suggested to mediate cellular responses to diverse stimuli, including ionizing radiation, growth factor stimulation, adhesion receptor engagement, and oxidative stress (5, 11, 14, 18, 25, 30). Abl and Arg kinase activities are normally kept under tight control in cells, but treatment with one of these stimuli can lead to a two- to fivefold increase in kinase activity. It is largely unknown how the membrane receptors and other cellular sensors of these stimuli interface with Abl and Arg to promote increased kinase activity.

The N-terminal halves of Abl and Arg have Src homology 3 (SH3), SH2, and tyrosine kinase domains in tandem. This modular structure is shared with Src family nonreceptor tyrosine kinases, suggesting that Abl and Src family kinases have similar regulatory mechanisms. Structural analysis reveals that Src family kinases are stabilized in an inactive conformation by two sets of intramolecular interactions (29, 36). The Src SH3 domain binds to a short linker between the SH2 and kinase domains, while the SH2 domain binds to an inhibitory phosphotyrosine (PY) residue near the C terminus. When engaged with their intramolecular targets, the SH3 and SH2 domains form a rigid frame that stacks along the back surface of the kinase domain and stabilizes Src in an inactive conformation (29, 36). Mutational disruption of either of these two interactions leads to activation of Src kinase activity (19, 24, 31).

Similar to Src, mutations of the Abl SH3 domain or its putative target in the SH2-kinase linker region lead to increased Abl kinase activity, suggesting that intramolecular contacts may help keep Abl in an inactive state (2, 10, 13). Recent studies reveal that the variable N-terminal domain of type IV Abl helps maintain Abl in an inactive conformation through interactions with the SH3-SH2-kinase domain module (26). The cellular antioxidant protein PAG can also bind to the Abl SH3 domain and inhibit kinase activity, suggesting that it may help keep Abl inactive through interactions with the SH3 domain (34). It is unclear, however, whether the SH2 domain of Abl or Arg engages in interactions that help keep the kinase in the inactive state.

Activation of Src family nonreceptor tyrosine kinases requires both breakdown of the inhibitory interactions and rearrangement of the kinase domain into an active conformation. Strong ligands for the Src SH3 or SH2 domain activate Src kinase activity, presumably by releasing the SH3 and SH2 domains from their inhibitory lock on the kinase domain (1, 22). When Src family kinases are active, residues in helix C form part of the kinase active site (37). Assembly of the kinase active site is controlled by tyrosine phosphorylation of an activation loop that connects the N- and C-terminal lobes of the kinase domain. In inactive Src, this central part of the activation loop inserts between the N- and C-terminal lobes of the kinase domain, occluding access to the active site and pushing helix C out of position relative to other residues in the active site (28, 35). Phosphorylation of a conserved tyrosine in the loop (Y416 in Src) reorients the activation loop, allowing substrates access to the active site and permitting helix C to rotate into position to form the active site (37).

Tyrosine phosphorylation is also a critical regulatory event in Abl family kinase activation, but it is unclear exactly how this phosphorylation is achieved. Abl has been reported to autophosphorylate in *trans* at two sites in vitro: Y245 in the SH2 domain-kinase linker and Y412 in the activation loop (4). Autophosphorylation at both sites contributes to Abl kinase ac-

* Corresponding author. Mailing address: Yale School of Medicine, SHMC-E31, 333 Cedar St., New Haven, CT 06520. Phone: (203) 785-5624. Fax: (203) 785-7979. E-mail: anthony.koleske@yale.edu.

tivity (4). Other experiments show that expression of an activated Src mutant (Src527F) with Abl in HEK293 cells leads to increased tyrosine phosphorylation of Abl and increased Abl kinase activity (8, 25). An increase in tyrosine phosphorylation is not observed on an Abl412F activation loop mutant upon coexpression with Src527F, and the Abl412F mutant is resistant to activation by Src527F (8). Together, these data suggest that Src can mediate activation of Abl by promoting phosphorylation of Y412 in the Abl activation loop. These experiments collectively suggest that two phosphorylation pathways can activate Abl: (i) Abl can activate itself through autophosphorylation and (ii) Abl can be activated through phosphorylation by Src.

We report here a comparison of the two pathways for Abl family kinase activation using purified recombinant proteins. We confirm that Abl and Arg are both activated by autophosphorylation at several sites. This activation can be further enhanced through direct phosphorylation by the Src family kinase Hck. Unexpectedly, autoactivation requires phosphorylation at sites that are distinct from those required for Hck-mediated stimulation. Autoactivation of Abl and Arg does not require phosphorylation of the activation loop tyrosines, whereas Hck directly stimulates Abl/Arg activity by phosphorylating Y412 and Y439 in the activation loop. We propose that the autoactivation pathway may allow Abl family kinases to amplify or integrate stimulatory cues relayed from cell surface receptors by Src family kinases.

MATERIALS AND METHODS

Production of recombinant proteins. Full-length Abl/Arg and Abl/Arg mutant cDNAs were constructed by PCR using murine Abl/Arg cDNA as the template. Amino acids are numbered as for the myristoylated form of murine Abl/Arg. With the exception of the ΔSH3 and "capped" variants of Abl and Arg, our constructs lack the variable N-terminal domain and begin with the first common exon (E46 in myristoylated Abl and E74 in myristoylated Arg). Wild-type and mutant cDNAs were cloned into the pFastBac HTa plasmids, except for ΔSH3 and Cap Abl/Arg, which were C terminally His tagged and cloned into pFastBas1. Abl/Arg proteins were produced with the Bac-to-Bac expression system (Life Technologies). For protein expression, Hi-5 insect cells were infected with recombinant baculovirus at a multiplicity of infection of 0.5 and harvested after 48 h. The cells were lysed with a French press in 50 mM HEPES (pH 7.25), 5 mM β-mercaptoethanol, 500 mM KCl, 0.01% Nonidet P-40, 5% glycerol, and protease inhibitors (10 μg of pepstatin A/ml, 10 μg of chymostatin/ml, 10 μg of leupeptin/ml, 1 mM benzamidine, 50 μg of aprotinin/ml, 1 mM phenylmethylsulfonyl fluoride). The lysates were centrifuged at 100,000 × *g* for 1 h, and the supernatant was incubated with Ni-nitrilotriacetic acid resin (Qiagen) for 1 h. After extensive washing, protein was eluted with 20 mM HEPES (pH 7.25), 500 mM KCl, 0.01% Nonidet P-40, 5% glycerol, 5 mM β-mercaptoethanol, protease inhibitors, and 100 mM imidazole. Protein concentrations were determined by the Bradford assay (Bio-Rad). GST-Crk II (a gift from Bruce Mayer) and GST-Crk(120-225) (a gift from Ruibao Ren) were expressed and purified as described previously (14). The synthetic peptide substrate (AAVIYAAPFA KKK) was a gift from John Colicelli.

Autophosphorylation reactions. Phosphorylation reaction mixtures contained 20 mM HEPES (pH 7.25), 100 mM KCl, 15 mM $MgCl_2$, 15 mM $MnCl_2$, 1 mM dithiothreitol, 5% glycerol, 1 mM sodium orthovanadate, 100 μM ATP, and 0.7 μM Abl or Arg. Where specified, 500 nM Hck (a gift from John Kuriyan) was included in the reaction mixture. All reaction mixtures were incubated at 30°C for the same length of time. Autophosphorylation was initiated at various times by the addition of ATP, and the reactions were terminated after equal total periods of incubation at 30°C by the addition of ice-cold sodium dodecyl sulfate (SDS) sample buffer. The samples were resolved by SDS-polyacrylamide gel electrophoresis (PAGE), transferred to nitrocellulose, and probed with antibodies to PY (4G10; Upstate Biotechnology), Abl (Ab-3; Calbiochem), or Arg (15) to control for loading. Radioactive autophosphorylation reactions were conducted similarly, with the addition of 0.5 μCi of [γ-^{32}P]ATP. After being resolved by SDS-PAGE, the gels were exposed for autoradiography and quantitated using a Molecular Dynamics PhosphorImaging system and ImageQuant software.

In vitro kinase assays. Kinase assay mixtures contained 25 mM Tris (pH 7.25), 100 mM NaCl, 5 mM $MgCl_2$, 5 mM $MnCl_2$, 1 mM dithiothreitol, 5% glycerol, 100 ng of bovine serum albumin/μl, 1 mM sodium orthovanadate, and 7 nM kinase. After a 5-min preincubation at 30°C, 25-μl reactions were initiated by the addition of 500 nM GST-Crk II (unless stated otherwise), 5 μM ATP, and 0.5 μCi of [γ-^{32}P]ATP. The reactions were terminated after 30 s (unless stated otherwise) by the addition of ice-cold SDS sample buffer and were resolved by SDS-PAGE. The gels were dried, exposed for autoradiography, and quantitated using a Molecular Dynamics PhosphorImaging system and ImageQuant software.

Autophosphorylation and kinase assays. In order to measure changes in the kinase activity of Abl/Arg with autophosphorylation, at various times autophosphorylation reaction mixtures were diluted 100-fold into 30°C kinase buffer already containing ATP and substrate. Kinase assays were then conducted as described above.

In vivo kinase assays. p190RhoGAP and Abl or Arg were coexpressed in HEK293 cells in the presence of various concentrations of STI571 or solvent (dimethyl sulfoxide [DMSO]) alone as a control. After a 24-h incubation with STI571, the cells were lysed in SDS sample buffer. The lysates were resolved by SDS-PAGE, transferred to nitrocellulose, and probed with antibodies to PY (4G10) to measure the extent of p190RhoGap phosphorylation. The blots were subsequently stripped and reprobed for p190RhoGAP (Upstate Biotechnology) and Abl/Arg to control for expression levels. The blots were digitized and quantitated using NIH Image.

Phosphopeptide mapping. Abl and Arg were autophosphorylated as described above with the addition of 0.3 μCi of [γ-^{32}P]ATP/μl; 7.5 μg of the phosphorylated kinase was then resolved by SDS-PAGE and transferred to nitrocellulose. The blots were stained with Ponceau-S, and the Abl/Arg bands were excised. Tryptic peptides were prepared and resolved by Hunter thin-layer electrophoresis (pH 1.9) followed by chromatography as described previously (3). Two-dimensional (2-D) phosphoamino acid analysis was performed as described previously (7).

RESULTS

Preparation of nonactivated forms of Abl and Arg. Immunoblotting with anti-PY antibodies revealed that Abl and Arg contained significant PY when the kinases were purified from insect cells (Fig. 1A). To reduce autophosphorylation of Abl and Arg during expression, we screened several kinase inhibitors for the ability to inhibit Abl and Arg kinase activity. The tyrosine kinase inhibitor PD180970 (16) potently inhibited the kinase activities of Abl and Arg in vitro, with similar 50% inhibitory concentrations (IC_{50}s) (≈20 nM) and K_is (≈2 nM) for both kinases (Fig. 1B and C). Abl and Arg kinase activities were also similarly sensitive to the antileukemia drug STI571 ($IC_{50} \approx 650$ nM and $K_i \approx 60$ nM) (Fig. 1B and D) and to four other STI571-like 2-aminophenylpyrimidine compounds in vitro (Fig. 1B and Table 1). Expression of Abl or Arg with the 190-kDa GTPase-activating protein for Rho (p190RhoGAP) in HEK293 cells leads to increased PY levels on p190RhoGAP (S. E. Hernandez, J. Settleman, and A. J. Koleske, submitted for publication). Using this assay to monitor Abl and Arg kinase activity, we found that STI571 inhibits Abl and Arg kinase activities with similar IC_{50}s (≈300 nM) in vivo (Fig. 1E).

PD180970 has been shown to inhibit both Src family kinases and Abl family kinases (16). We included 30 μm PD180970 during expression of Abl or Arg to minimize both autophosphorylation and phosphorylation by endogenous tyrosine kinases in the insect cells. The Abl and Arg purified following expression with PD180970 contained no detectable PY, as revealed by immunoblotting with a cocktail containing the 4G10, PY20, and PY99 antibodies (Fig. 1A) and by mass spectrometry (data not shown). We will refer to these as nonactivated forms of Abl and Arg because they had 9- and 15-fold-reduced

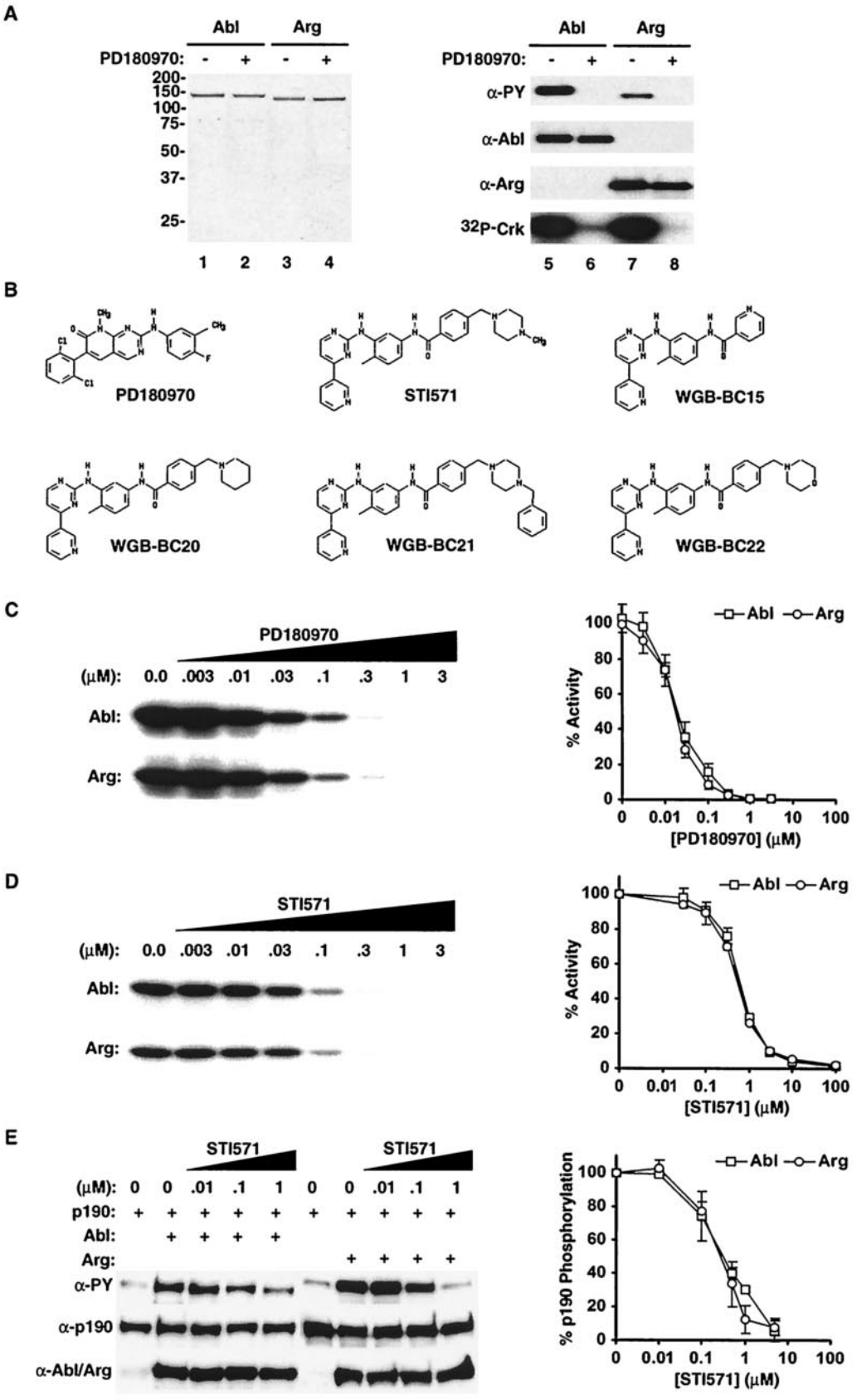
A
Abl
Arg
PD180970: - + - +
200-
150-
100-
75-
50-
37-
25-
1 2 3 4
Abl
Arg
PD180970: - + - +
α-PY
α-Abl
α-Arg
32P-Crk
5 6 7 8
B
PD180970
STI571
WGB-BC15
WGB-BC20
WGB-BC21
WGB-BC22
C
PD180970
(μM): 0.0 .003 .01 .03 .1 .3 1 3
Abl:
Arg:
Abl
Arg
% Activity
[PD180970] (μM)
D
STI571
(μM): 0.0 .003 .01 .03 .1 .3 1 3
Abl:
Arg:
Abl
Arg
% Activity
[STI571] (μM)
E
STI571
STI571
(μM): 0 0 .01 .1 1 0 0 .01 .1 1
p190: + + + + + + + + + +
Abl: + + + + +
Arg: + + + +
α-PY
α-p190
α-Abl/Arg
Abl
Arg
% p190 Phosphorylation
[STI571] (μM)

kinase activities, respectively, relative to their tyrosine-phosphorylated counterparts expressed in the absence of PD180970 (Fig. 1A). We show below that the nonactivated forms of Abl and Arg can be reactivated via phosphorylation in vitro to levels comparable to those of the phosphorylated Abl and Arg expressed in the absence of PD180970.

Activation of Abl and Arg kinase activities by autophosphorylation. Nonactivated Abl and Arg underwent autophosphorylation when incubated at 30°C in the presence of Mg^{2+}/Mn^{2+} and ATP, as revealed by immunoblotting with anti-PY antibodies (Fig. 2A). Autophosphorylation was detected on both Abl and Arg after only 2.5 min of incubation, and the amount of autophosphorylation increased with increasing incubation time. We used glutathione *S*-transferase (GST)-Crk as a substrate to monitor how autophosphorylation affects Abl and Arg kinase activities. Following the addition of Mg^{2+}/Mn^{2+} and ATP, we observed time-dependent increases in Abl and Arg kinase activities. These increases plateaued at 30 min (Fig. 2B) and resulted in 5.2- or 6.2-fold activation of Abl or Arg kinase activity, respectively. Abl and Arg incubated in Mg^{2+}/Mn^{2+} without ATP or in ATP without Mg^{2+}/Mn^{2+} did not exhibit increased kinase activity (data not shown).

Autophosphorylation was also monitored independently by incubating nonactivated Abl and Arg in Mg^{2+}/Mn^{2+} and [γ-^{32}P]ATP and monitoring the transfer of radioactive phosphate to the kinases (Fig. 2C and D). We noted that Abl and Arg autophosphorylation levels continued to increase beyond 30 min, but this increased autophosphorylation did not promote further increases in kinase activity (Fig. 2B and D).

We reasoned that if nonactivated Abl and Arg could autophosphorylate during the course of the in vitro kinase assay, the activities of nonactivated Abl and Arg might increase during the assay. Indeed, we observed time-dependent increases in the activities of nonactivated Abl and Arg with increasing kinase assay length (Fig. 2E). As expected, Abl and Arg that had been previously autoactivated did not exhibit increased activity during the assay (Fig. 2E). Because the nonactivated kinases autoactivate during the kinase assay, the observed difference between the kinase activities of nonactivated and autoactivated Abl and Arg decreases with assay duration (Fig. 2F). We observed a maximum of 5.2- and 6.2-fold autoactivation of Abl and Arg, respectively, using a 30-s kinase assay. We therefore monitored kinase activity using 30-s kinase assays unless stated otherwise.

We next determined whether autophosphorylation affects the catalytic rate (k_{cat}) or substrate affinity (K_m) of Abl or Arg for a variety of substrates. We monitored how the kinase activities of nonactivated or autophosphorylated Abl or Arg varied with the substrate concentration and determined the K_m and k_{cat} of each kinase preparation by analyzing the data on double reciprocal plots (1/velocity versus 1/[substrate]). Autophosphorylated Abl and Arg had five- and sixfold increases in the k_{cat} for GST-Crk, respectively, compared to their nonactivated counterparts (Table 2). Autophosphorylation did not appreciably affect the K_ms of Abl or Arg for GST-Crk (Table 2). We observed 4.5- and 6.1-fold enhancements in catalytic efficiency (the increase in k_{cat}/K_m) upon autophosphorylation of Abl and Arg, respectively.

Although the 30-s assays allowed us to measure phosphorylated GST-Crk at high concentration, we had difficulty detecting phosphorylated products in reactions containing low concentrations of GST-Crk. This limited our ability to measure K_ms accurately, because we could not obtain data from lower substrate concentrations. We therefore used 5-min kinase assays to more accurately measure the K_ms of Abl and Arg for GST-Crk (Fig. 3 and Table 2). As observed in the 30-s assays, autophosphorylation increased the k_{cat} values of Abl and Arg on GST-Crk. As expected, the k_{cat} values of nonactivated Abl and Arg were higher when measured in the 5-min assay than in the 30-s assay as a result of autophosphorylation occurring during the longer kinase assay. Autophosphorylation had no effect on the K_m of Abl or Arg for GST-Crk. Moreover, the K_ms of Abl or Arg for GST-Crk determined by either method were similar (Table 2).

We used 5-min kinase assays to compare the kinase activities of nonactivated and autoactivated Abl and Arg on several additional test substrates, including a shortened version of

TABLE 1. In vitro drug sensitivities of nonactivated Abl and Arg

Drug	IC_{50} (μM)[a]	
	Abl	Arg
PD180970	0.022 ± .003	0.019 ± 0.004
STI571	0.62 ± 0.04	0.69 ± 0.04
WGB-BC15	2.0 ± 0.5	2.0 ± 0.5
WGB-BC20	3 ± 1	0.9 ± 0.3
WGB-BC21	0.7 ± 0.2	0.9 ± 0.2
WGB-BC22	3.0 ± 0.8	2.0 ± 0.5

[a] Mean ± standard error; $n = 4$.

FIG. 1. Purification of Abl and Arg lacking PY. (A) Abl (lanes 1 and 2) and Arg (lanes 3 and 4) were purified after expression in the absence (−) (lanes 1 and 3) or presence (+) (lanes 2 and 4) of PD180970. Five micrograms of each purified protein was separated by SDS-PAGE and visualized by staining with Coomassie brilliant blue; 80 ng of Abl (lanes 5 and 6) or Arg (lanes 7 and 8) purified in the absence (lanes 5 and 7) or presence (lanes 6 and 8) of PD180970 was immunoblotted with antibodies (α) to PY (right, top). The blots were stripped and reprobed with antibodies to Abl (right, second from top) or Arg (right, second from bottom) to control for the amount loaded. The relative kinase activities of these purified proteins toward the GST-Crk substrate are shown (right, bottom). (B) Chemical structures of PD180970 and the 2-aminophenylpyrimidine derivatives. (C) Nonactivated Abl (top) and Arg (bottom) kinase activities toward GST-Crk in the presence of increasing concentrations of PD180970. Each data point is the mean of three independent measurements and is normalized to a control sample containing DMSO alone. The error bars represent standard errors. (D) Nonactivated Abl (top) and Arg (bottom) kinase activities (mean ± standard error; $n = 3$) toward GST-Crk in the presence of increasing concentrations of STI571 normalized to a DMSO control. (E) HEK293 cells expressing p190RhoGAP alone or p190RhoGAP plus Abl or Arg were incubated with increasing concentrations of STI571. Total cell lysates were probed for PY (top). The blots were stripped and reprobed with antibodies to p190RhoGAP (middle) and Abl or Arg (bottom) to control for expression levels. The PY blots were digitized and quantitated as a measure of Abl and Arg activities. The data (mean ± standard error; $n = 3$) are normalized to a DMSO control.

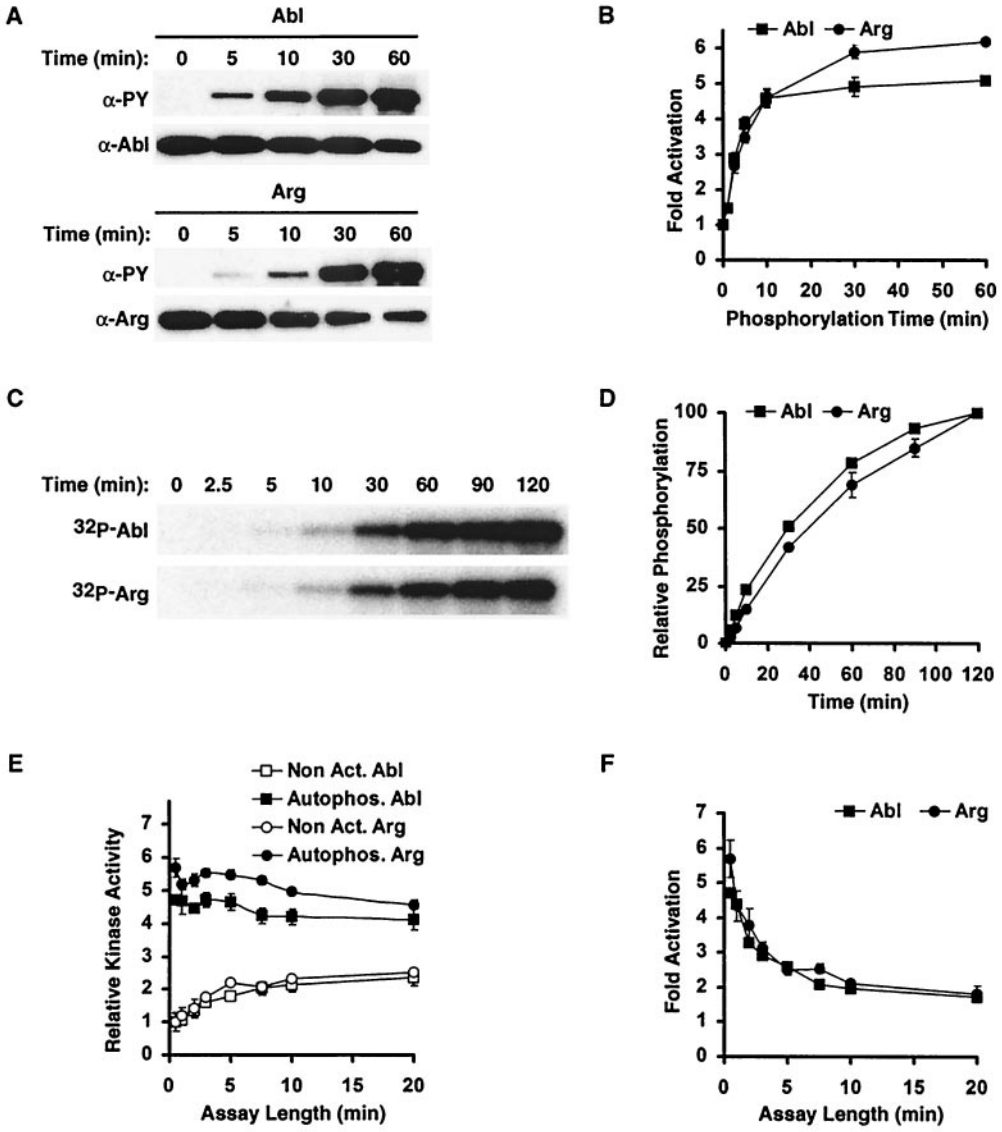

FIG. 2. Abl and Arg are activated by autophosphorylation. (A) Nonactivated Abl and Arg (700 nM) were incubated in ATP and Mg^{2+}/Mn^{2+}. After increasing times of incubation, 80 ng was immunoblotted and probed for anti-PY and anti-Abl or Arg, as indicated. (B) Abl and Arg kinase activities on GST-Crk after increasing times of autophosphorylation; *n*-fold activation (mean ± standard error; $n = 3$) above nonactivated Abl and Arg is shown. (C) Nonactivated Abl and Arg (700 nM) were incubated in [γ-^{32}P]ATP and Mg^{2+}/Mn^{2+}, and autophosphorylated Abl/Arg was visualized by autoradiography. (D) Relative amounts of tyrosine phosphorylation (mean ± standard error; $n = 3$) on Abl or Arg with increasing times of autophosphorylation. (E) Kinase activities (mean ± standard error; $n = 3$) of Abl and Arg before (Non Act) and after (Autophos) a 60-min autophosphorylation reaction were monitored using increasing kinase assay times. (F) *n*-Fold activation of autophosphorylated Abl and Arg (mean ± standard error; $n = 3$) above the nonactivated kinases observed using increasing kinase assay times.

GST-Crk (GST-Crk110-225) and a synthetic peptide substrate sequence (14) (Table 2). Autophosphorylation increased the k_{cat} values of Abl and Arg for each substrate but had no effect on the substrate K_ms (Table 2). The increased k_{cat} upon autophosphorylation was more pronounced for some substrates than others. Autophosphorylation promoted the largest enhancements of catalytic rates on the GST-Crk substrate.

Abl and Arg autophosphorylate at two or more sites. We analyzed the autophosphorylation sites in Abl and Arg to better understand how phosphorylation promotes increased Abl and Arg kinase activities. Abl was allowed to autophosphorylate in vitro with [γ-^{32}P]ATP and was digested with trypsin. The resulting peptides were separated by 2-D chromatography. This analysis identified three predominant phosphorylated peptides for Abl, which we refer to as "b" peptides (for Abl): bA, bB, and bC (Fig. 4B). Similar experiments identified six major phosphopeptide-containing spots for Arg, which we refer to as "r" peptides (for Arg): rA, rB, rC, rD, rE, and rF (Fig. 4C). Because trypsin does not digest Abl and Arg to completion, it is possible to obtain more than one phosphopeptide for a single phosphorylation site. Phosphoamino acid analysis of autophosphorylated Abl and Arg indicated that phosphate was incorporated on tyrosine only during the autophosphorylation reactions (data not shown).

TABLE 2. Abl and Arg have similar enzymatic properties

Assay	Kinase	Substrate	Results[a]										
			k_{cat} (min^{-1})			K_m (μM)			k_{cat}/K_m (min^{-1} μM^{-1})			Fold $\Delta k_{cat}/K_m$[b]	
			Nonact.	Autophos.	Hck Act.	Nonact.	Autophos.	Hck Act.	Nonact.	Auto.	Hck Act.	Auto.	Hck Act.
30 s	Abl	GST-Crk	0.07 ± 0.01	0.35 ± 0.05	0.8 ± 0.2	0.18 ± 0.05	0.20 ± 0.05	0.3 ± 0.2	0.39	1.75	2.7	4.5	6.9
	Arg	GST-Crk	0.04 ± 0.05	0.23 ± 0.02	0.5 ± 0.2	0.17 ± 0.1	0.15 ± 0.6	0.3 ± 0.2	0.25	1.53	1.7	6.1	6.6
5 min	Abl	GST-Crk	0.17 ± 0.02	0.33 ± 0.06	0.8 ± 0.2	0.19 ± 0.03	0.24 ± 0.04	0.5 ± 0.3	0.89	1.375	1.6	1.54	1.80
		GST-Crk(120-225)	0.09 ± 0.01	0.13 ± 0.01	ND	3.1 ± 0.2	2.9 ± 0.3	ND	0.029	0.045	ND	1.54	ND
		Peptide[c]	0.33 ± 0.06	0.65 ± 0.09	ND	27 ± 6	29 ± 1	ND	0.012	0.022	ND	1.83	ND
		ATP[d]	0.09 ± 0.01	ND	ND	0.9 ± 0.1	ND	ND	0.07	ND	ND	ND	ND
	Arg	GST-Crk	0.09 ± 0.01	0.22 ± 0.01	0.5 ± 0.1	0.24 ± 0.08	0.18 ± 0.01	0.5 ± 0.01	0.38	1.243	1.0	3.31	2.6
		GST-Crk(120-225)	0.06 ± 0.01	0.10 ± 0.01	ND	4.47 ± 0.08	6.0 ± 0.8	ND	0.013	0.017	ND	1.24	ND
		Peptide[c]	0.75 ± 0.08	1.10 ± 0.04	ND	123 ± 2	149 ± 8	ND	0.006	0.007	ND	1.21	ND
		ATP[d]	0.07 ± 0.01	ND	ND	0.7 ± 0.1	ND	ND	0.1	ND	ND	ND	ND

[a] Mean ± standard error; $n = 4$. ND, not determined; Act., activated; Autophos. or Auto., autophosphorylated.
[b] n-Fold change in catalytic efficiency with autophosphorylation.
[c] Peptide, AAVIYAAPFAKKK.
[d] GST-Crk(120-225) as substrate.

Brasher and Van Etten have shown that autophosphorylation of Abl at tyrosine 245 in the SH2-kinase domain linker and at tyrosine 412 in the activation loop both promote kinase activation (Fig. 4A) (4). We made nonphosphorylatable phenylalanine (F) substitution mutations at these sites either alone (245F or 412F) or in combination (245F/412F). Following autophosphorylation in vitro, these mutants were subjected to 2-D phosphopeptide mapping. We detected no phosphopeptide at positions bB and bC in the 2-D map of Abl245F, although the phosphopeptide at position bA appeared normally (Fig. 4D). The 2-D map of the Abl412F mutant showed a pattern identical to that of wild-type Abl, with phosphopeptide spots bA, bB, and bC (Fig. 4F). These data indicated that the phosphopeptides bB and bC represented autophosphory-

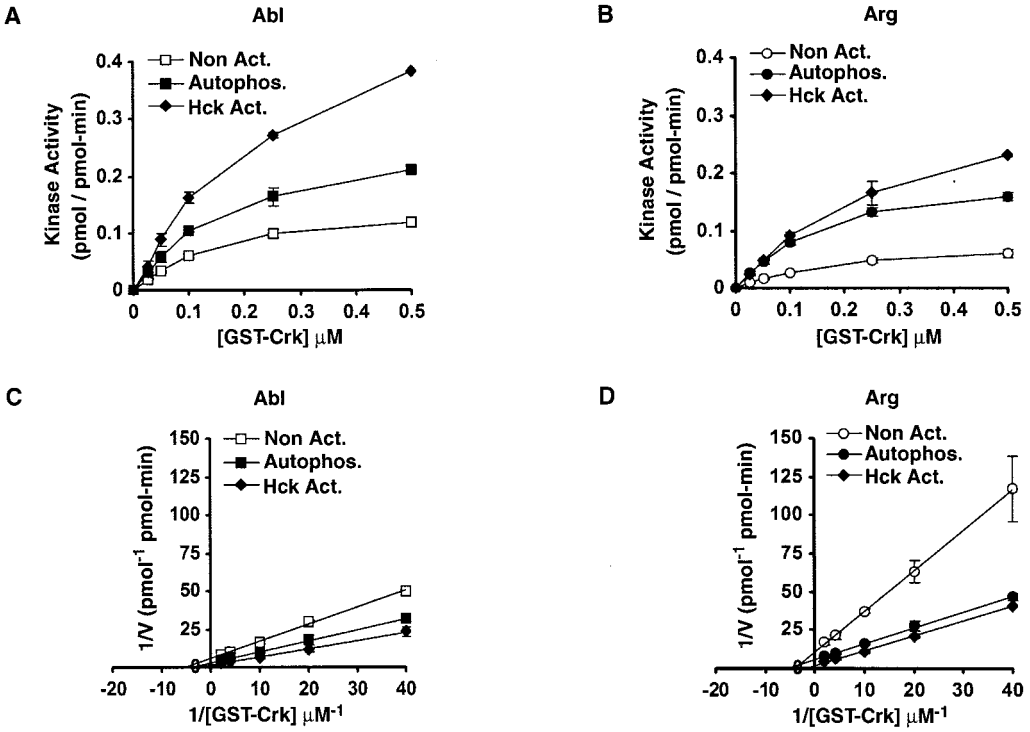

FIG. 3. Autophosphorylation and Hck phosphorylation increase the catalytic rates of Abl and Arg. (A) Kinase activities (mean ± standard error; $n = 4$) of Abl before (Non Act.) and after (Autophos.) a 60-min autophosphorylation reaction or a 60-min autophosphorylation reaction including Hck (Hck Act.) were measured with 5-min kinase assays in the presence of increasing GST-Crk concentrations. (B) Kinase activities (mean ± standard error; $n = 4$) of Arg before (Non Act.) and after (Autophos.) a 60-min autophosphorylation reaction or a 60-min autophosphorylation reaction including Hck (Hck Act.) were measured with 5-min kinase assays in the presence of increasing GST-Crk concentrations. (C) Double reciprocal Lineweaver-Burk plots of the data in panel A. (D) Double reciprocal Lineweaver-Burk plots of the data in panel B.

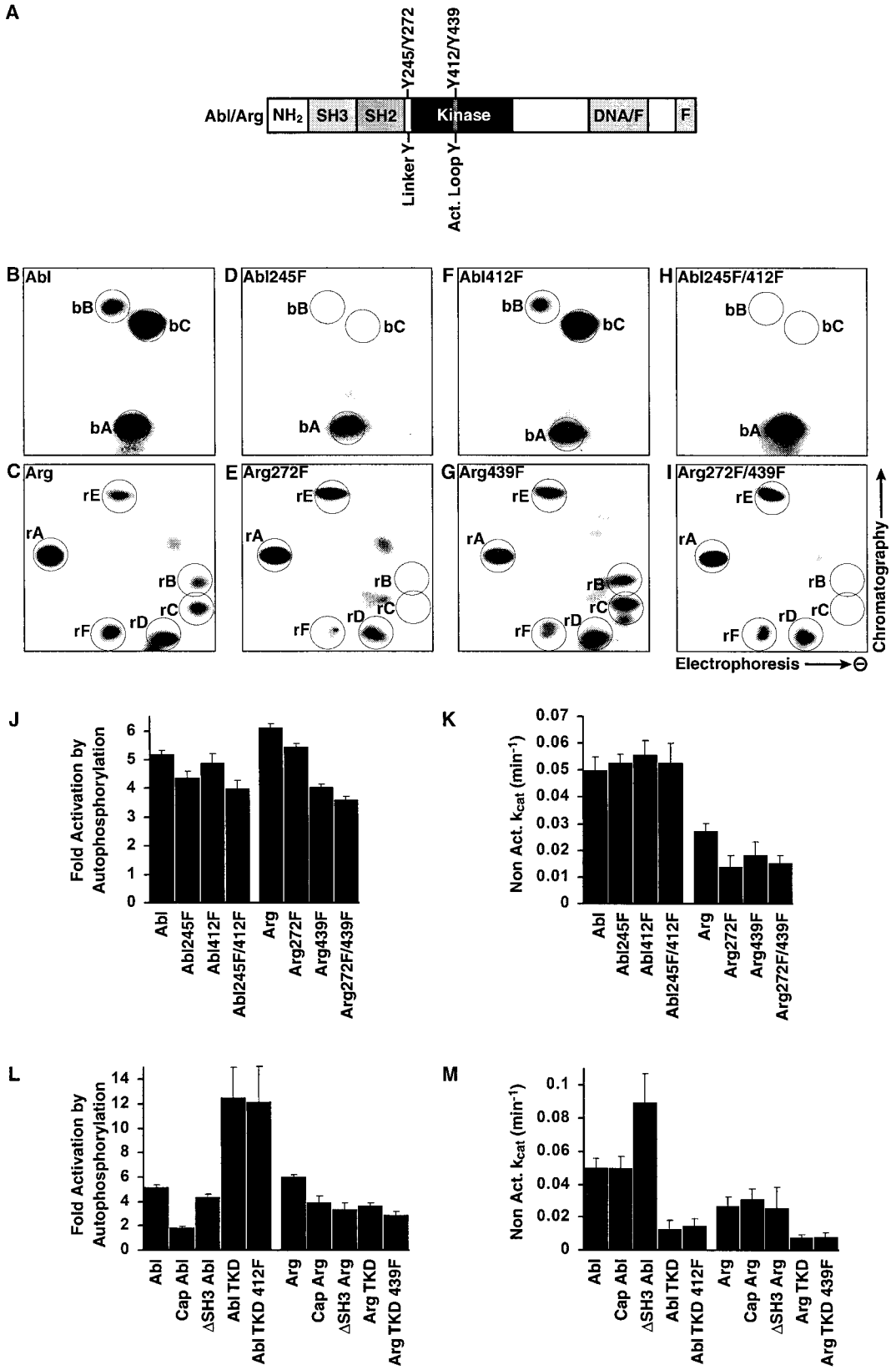

FIG. 4. Abl and Arg are activated by autophosphorylation on novel sites. (A) Schematic of Abl and Arg indicating the arrangement of the SH3, SH2, kinase, and F-actin binding (F) domains. The DNA/F region of Abl binds DNA (21), whereas the corresponding region in Arg binds F-actin (33). The locations of the linker tyrosine (Abl Y245 and Arg Y272) and activation loop tyrosine (Abl Y412 and Arg Y439) are shown. (B to I) Tryptic digests of autophosphorylated Abl and Arg were separated by electrophoresis in the lateral direction, followed by thin-layer chromatography in

lation at Y245 and that Y412 was not detectably autophosphorylated by nonactivated Abl. In further support of this assignment, the 2-D map of the double mutant Abl245F/412F lacked phosphopeptides bB and bC (Fig. 4H).

We also mutated the corresponding residues in Arg, Y272 and Y439 (Fig. 4A), to determine whether these sites are targeted by autophosphorylation. Following autophosphorylation, trypsin digestion, and 2-D separation of Arg272F, we detected no phosphopeptides at positions rB and rC in the 2-D map (Fig. 4E), although the other phosphopeptides appeared normally. The phosphopeptide map of the Arg439F mutant was identical to the phosphopeptide map of wild-type Arg (Fig. 4G). These data suggest that phosphopeptides rB and rC represent autophosphorylation at position Y272 and that Y439 was not detectably autophosphorylated by nonactivated Arg. A 2-D map of the Arg272F/439F double mutant lacked both peptides rB and rC (Fig. 4I), in agreement with our peptide assignments.

To confirm the phosphorylation sites indicated by the peptide mapping experiments and to identify the remaining autophosphorylation sites in Abl and Arg, nonactivated and autoactivated Abl/Arg were digested with trypsin, and phosphopeptides were identified and sequenced by nanoelectrospray tandem mass spectrometry. In agreement with the data described above, we detected autophosphorylation of the linker tyrosines but not the activation loop tyrosines (data not shown). We also found that two tyrosines unique to Arg, Y568 and Y684, were autophosphorylated. Phosphopeptide maps of Arg568F and Arg684F indicated that these are major autophosphorylation sites that correspond to spots rA and rE, respectively (data not shown). Despite repeated attempts, we did not identify the phosphorylation sites corresponding to Abl phosphopeptide spot bA or Arg phosphopeptide spots rD and rF by mass spectrometry.

Autoactivation can occur independently of the linker and activation loop tyrosines. We next determined whether autophosphorylation of the SH2-kinase domain linker tyrosines contributes to kinase activation. As noted above, Abl and Arg are activated 5.2- and 6.2-fold, respectively, by autophosphorylation (Fig. 4J). Mutation of the SH2-kinase linker tyrosines resulted in a modest but reproducible decrease in kinase autoactivation. The Abl245F and Arg272F mutants were activated 4.4- and 5.5-fold in vitro, respectively (Fig. 4J). The nonactivated forms of these mutants had catalytic rates comparable to those of the wild-type enzymes, suggesting that these mutations did not lead to gross structural perturbations of the kinase domains (Fig. 4K).

Previous studies have shown that autophosphorylation of the activation loop tyrosine stimulates Abl kinase activity (4). Unexpectedly, we found that mutation of this site to phenylalanine did not significantly affect Abl kinase activation. The Abl412F mutant was activated 4.9-fold by autophosphorylation, comparable to the 5.2-fold autoactivation observed for wild-type Abl (Fig. 4J). The corresponding Arg439F mutant was activated 4.1-fold by autophosphorylation (compared to 6.2-fold for wild-type Arg), suggesting that activation loop phosphorylation contributed modestly to Arg autoactivation. The basal kinase activities of these mutants were comparable to those of their respective wild-type counterparts (Fig. 4K). In addition, a double mutant of both the activation loop tyrosine and the SH2-kinase linker domain tyrosines also had only a modest effect on autoactivation. The Abl245F/412F and Arg272F/439F mutants could autoactivate 4.0- and 3.7-fold, respectively, and their basal activities were comparable to those of the wild-type enzymes (Fig. 4J and K). We conclude that Abl and Arg can autoactivate independently of the linker and activation loop tyrosines.

We also examined whether autophosphorylation of Y568 or Y684 in Arg is important for autoactivation of Arg. Mutation of these residues to phenylalanine has no effect on Arg autoactivation (data not shown).

In order to find the minimal region required for autoactivation, we tested the abilities of several deletion mutants of Abl and Arg to autoactivate. We found that only the kinase domain is required for autoactivation, and like the full-length proteins, the activation loop tyrosines are not required for autoactivation of the Abl and Arg kinase domains (Fig. 4L).

Abl and Arg kinase activities are increased by the Src family kinase Hck. Src family kinases phosphorylate Abl family kinases in vitro and in vivo (11, 25, 27). Indeed, when included with Abl or Arg in a 1-h activation reaction, the Src family kinase Hck promoted 10.3- and 12.6-fold activation of Abl and Arg, respectively (Fig. 5A and B). These levels represent additional 2.0-fold increases above the autoactivated kinase activity of Abl and Arg. Hck had no stimulatory effect when ATP was not included in an Abl/Arg phosphorylation reaction prior to the kinase assay (Fig. 5A and B). We monitored how the kinase activities of Hck-phosphorylated and autophosphorylated Abl and Arg varied with the GST-Crk concentration. This analysis indicated that Hck phosphorylation increased the k_{cat}s of Abl and Arg 2.4- and 2.3-fold, respectively, but raised their K_m values for GST-Crk 1.5- and 2.0-fold, respectively (Fig. 3 and Table 2). This increased K_m for GST-Crk explains why the stimulatory effects of Hck are reduced at lower substrate concentrations (Fig. 3A and B).

We mapped the Hck phosphorylation sites in Abl and Arg to better understand how Hck phosphorylation promotes increased Abl and Arg kinase activity. Nonactivated Abl and Arg

the vertical direction. This revealed three major phosphorylated tryptic peptides for Abl (spots bA, bB, and bC) (B) and six major phosphorylated tryptic peptides for Arg (spots rA, rB, rC, rD, rE, and rF) (C). Phosphopeptide maps for Arg also contained a few spots of lower intensity (unlabeled) that varied in appearance between experiments. Similar experiments were done using Abl245F (D), Arg272F (E), Abl412F (F), Arg439F (G), Abl245F/412F (H), and Arg272F/439F (I). (J) The *n*-fold activation (mean plus standard error; $n \geq 3$) of Abl, Arg, and the linker-activation loop tyrosine mutants was measured after 60 min of autophosphorylation. (K) Nonactivated catalytic rates (means plus standard errors; $n \geq 3$) of the Abl, Arg, and phosphorylation site mutants. (L) The *n*-fold activation (mean plus standard error; $n \geq 3$) of Abl and Arg lacking the N-terminal domain (Abl and Arg), containing the N-terminal domain (Cap Abl and Cap Arg), or the isolated Abl and Arg kinase domains (Abl TKD and Arg TKD) was measured after 60 min of autophosphorylation. (M) Nonactivated catalytic rates (means plus standard errors; $n \geq 3$) of the domain mutants.

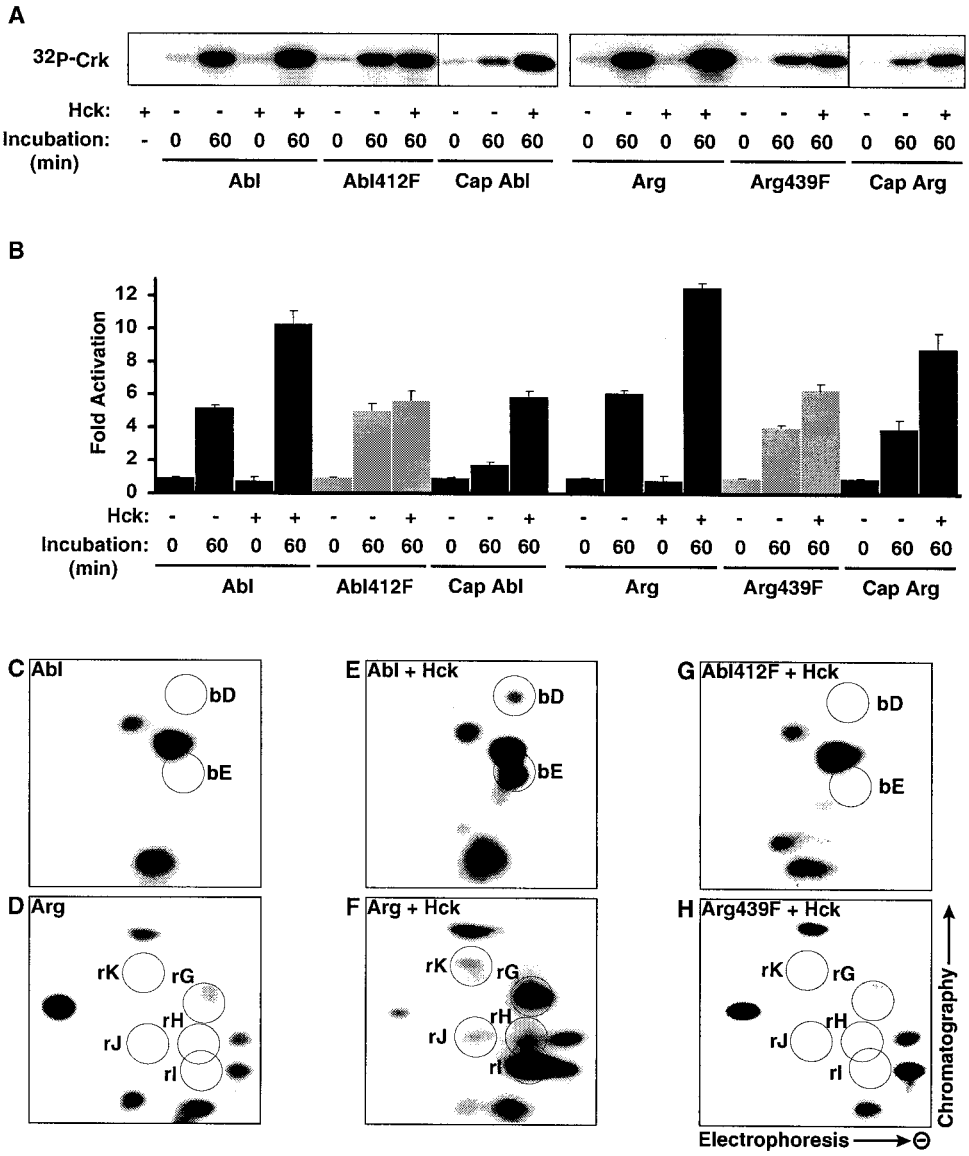

FIG. 5. Hck activates Abl and Arg by phosphorylating their activation loop tyrosines. (A) Abl, Abl412F, Cap Abl, Arg, Arg439F, and Cap Arg kinase activities on GST-Crk before or after 60 min of autophosphorylation in the absence (−) or presence (+) of Hck. A kinase assay containing Hck alone shows that Hck does not phosphorylate GST-Crk. (B) The *n*-fold activation (mean plus standard error; $n \geq 3$) relative to nonactivated kinase activity after 60 min of autophosphorylation in the absence (−) or presence (+) of Hck for Abl, Abl412F, Cap Abl, Arg, Arg439F, and Cap Arg. (C to H) Tryptic digests of Abl (C and E) and Arg (D and F) autophosphorylated in the presence (E and F) or absence (C and D) of Hck were separated by electrophoresis in the lateral direction and by thin-layer chromatography in the vertical direction. Hck phosphorylation leads to two additional spots for Abl (bD and bE) and five additional spots for Arg (rG, rH, rI, rJ, and rK). Mutation of Y412 in Abl (G) and Y439 in Arg (H) resulted in the disappearance of all additional spots.

were labeled with [γ-^{32}P]ATP in the presence or absence of Hck for 1 h and subjected to 2-D phosphopeptide analysis. Incubation of Abl or Arg alone led to the appearance of the expected phosphopeptide spots, as shown in Fig. 4 and 5C and D. Inclusion of Hck in these incubations led to the appearance of two novel spots for the Abl reaction (spots bD and bE) and five novel spots for the Arg reaction (spots rG, rH, rI, rJ, and rK) (Fig. 5E and F). These additional spots were missing from the Abl412F and Arg439F activation loop mutants, indicating that Hck directly phosphorylates Abl and Arg on these residues (Fig. 5G and H). We also used kinase-inactive mutants of Abl and Arg (Ablk290M and Argk317M) to determine whether Hck can target residues which are normally autophosphorylated by Abl and Arg during the phosphorylation reactions. This analysis revealed that Hck also directly phosphorylates the linker tyrosines of Abl and Arg, although less efficiently than the activation loop tyrosines (data not shown). However, Abl and Arg containing phenylalanine substitutions for the linker tyrosine are activated normally by Hck, indicating that the linker tyrosines are not required for activation by Hck (data not shown).

To test whether activation loop phosphorylation is required

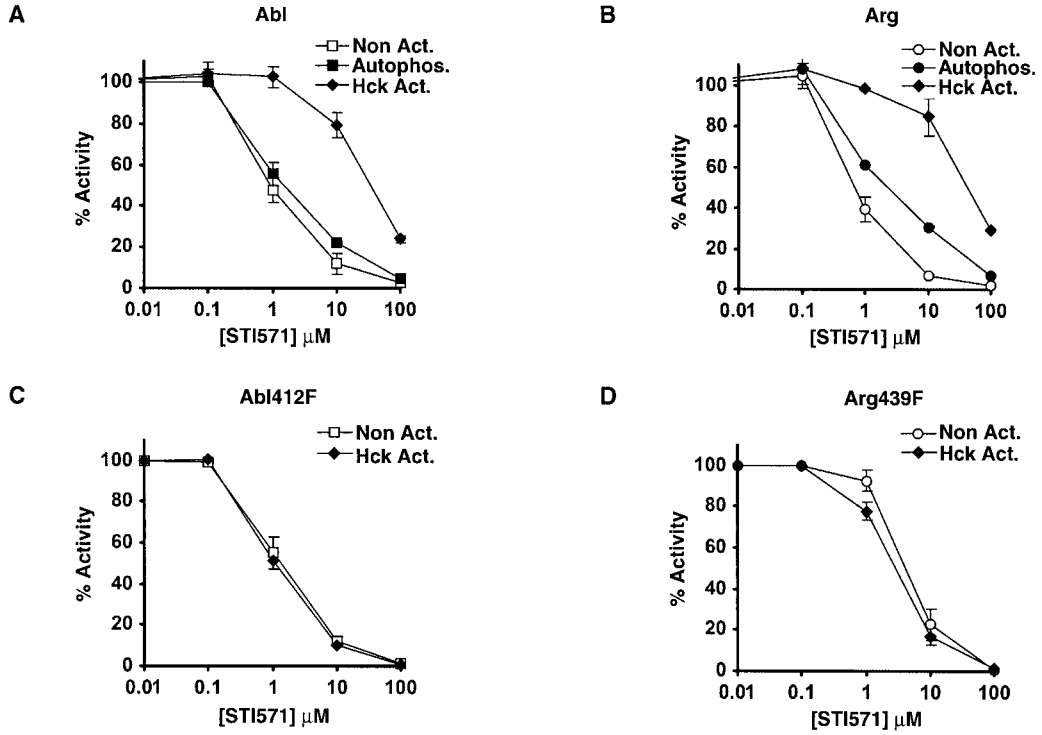

FIG. 6. Phosphorylation of activation loop tyrosines leads to STI571 resistance. (A and B) Kinase activities (mean ± standard error; $n = 3$) of nonactivated, autophosphorylated, and Hck-phosphorylated Abl (A) and Arg (B) on GST-Crk in the presence of increasing concentrations of STI571 normalized to a DMSO control. (C and D) Kinase activities (mean ± standard error; $n = 3$) of nonactivated and Hck-phosphorylated Abl412F (C) and Arg439F (D) on GST-Crk in the presence of increasing concentrations of STI571 normalized to a DMSO control.

for Hck to activate Abl and Arg, we examined whether Hck could activate the Abl412F and Arg439F mutants. Although Abl412F could autoactivate, we found that Hck did not promote further activation of its kinase activity (Fig. 5A and B). Similarly, Arg439F was only slightly activated by Hck (1.5-fold). Together with the peptide-mapping experiments, these data indicate that Hck directly activates Abl and Arg via phosphorylation of their activation loop tyrosines.

The N-terminal cap reduces autoactivation of Abl and Arg. The Abl and Arg proteins used in our study lacked the variable N-terminal domain which is reported to form an inhibitory "cap" on the SH3 and kinase domains (26). We analyzed whether the presence of the cap has an effect on autoactivation. Abl and Arg containing the N-terminal domain (Cap Abl and Cap Arg) retained the ability to autoactivate (1.9- and 4.0-fold, respectively), although to a lesser extent than Abl and Arg lacking the cap (Fig. 4L). Hck activated the cap-containing Abl and Arg 3.2- and 2.2-fold, respectively, over the autophosphorylated levels (Fig. 5A and B).

We also tested whether elimination of the SH3 domain, which is known to inhibit Abl kinase activity (2, 4, 10, 13), affects Abl or Arg activation. As expected, deletion of the SH3 domain enhanced Abl basal kinase activity (Fig. 4M). However, we observed no change in basal activity following deletion of this domain in Arg (Fig. 4M). Abl and Arg mutants lacking the SH3 domain exhibited a decreased ability to autoactivate (4.4- and 3.5-fold, respectively) (Fig. 4L).

Activation loop phosphorylation results in STI571 resistance. Phosphorylation of the Abl activation loop has been shown to reduce its sensitivity to STI571 (27). Indeed, we noted that the in vitro kinase activities of tyrosine-phosphorylated Abl and Arg expressed in the absence of PD180970 were less sensitive to STI571 than their nonphosphorylated counterparts. Autophosphorylation had no effect on the STI571 sensitivity of Abl and only a slight effect for Arg, confirming that Abl and Arg cannot efficiently phosphorylate their activation loops (Fig. 6A and B). In contrast, Abl and Arg were 50-fold less sensitive to STI571 after phosphorylation by Hck. The STI571 sensitivities of Abl412F and Arg439F were not changed by Hck phosphorylation. These data are in agreement with our finding that Hck phosphorylates the activation loops of Abl and Arg (Fig. 6C and D).

DISCUSSION

We report here that Abl and Arg can be activated through two distinct mechanisms: (i) Abl and Arg can each autophosphorylate, leading to increased kinase activity, and (ii) the Src family kinase Hck can further stimulate Abl and Arg by phosphorylating them on their activation loops.

Abl and Arg have similar enzymatic properties. Sequence comparisons and genetic analysis in mice suggest that Abl and Arg might have a functional overlap in cells (15, 17). Indeed, we found that Abl and Arg have very similar kinetic properties on three test substrates (Table 2). We also found that Abl and Arg are regulated similarly by autophosphorylation and by phosphorylation by Hck. These observations suggest that Abl and Arg may function in similar signaling pathways, supporting

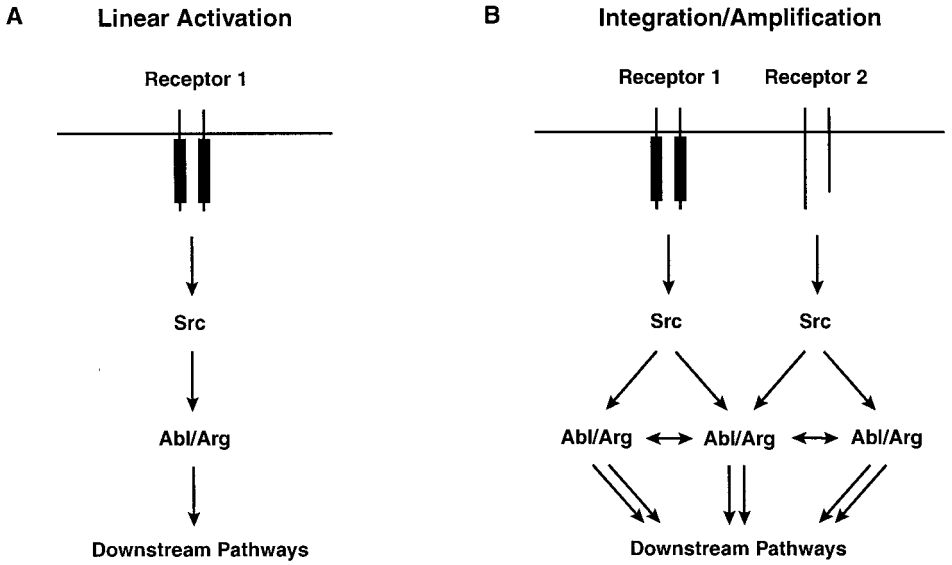

FIG. 7. Model for Abl family kinase activation. Both schemes depict models where an Src family kinase becomes activated by cell surface receptors. (A) When Abl or Arg (Abl/Arg) concentrations are low, an Src family kinase would activate Abl/Arg through phosphorylation of the activation loop, leading to modest linear activation of downstream pathways. (B) The outcome of this activation would change when the Abl/Arg concentration is elevated locally. Following phosphorylation of their activation loops by Src family kinases, Abl/Arg would activate nearby Abl/Arg molecules by phosphorylating tyrosines outside the activation loop. This amplification would lead to a more robust activation of downstream pathways. The autoactivation pathway would also allow Abl/Arg to integrate signals from distinct cell surface receptors.

the functional overlap observed in genetic experiments in mice (15).

Abl and Arg autoactivate by phosphorylating several residues. We report here that nonactivated Abl and Arg autophosphorylate on several tyrosine residues, leading to 5.2- and 6.2-fold increases in kinase activity, respectively. Both Abl and Arg can phosphorylate a tyrosine in the SH2-kinase domain linker (Y245 in Abl; Y272 in Arg), as previously reported for Abl (4). Mutation of this linker tyrosine to phenylalanine in Abl or Arg leads to only a slight reduction in their abilities to autoactivate, suggesting that phosphorylation of other sites is also required for autoactivation. Indeed, our phosphopeptide analysis shows that Abl and Arg autophosphorylate at one or more tyrosine residues in addition to the linker site. Further, the autoregulatory tyrosines are within the kinase domains of Abl and Arg. Phosphorylation of these unidentified kinase domain tyrosines likely contributes to the 4.4- and 5.5-fold activation observed for the Abl245F and Arg272F linker site mutants, respectively. Because our studies show that Abl and Arg have very similar enzymatic properties, we predict that the remaining activating autophosphorylation site(s) is shared between Abl and Arg and that phosphorylation leads to activation via similar mechanisms for both Abl and Arg.

Brasher and Van Etten (4) have previously reported that Abl autoactivates through phosphorylation of both the activation loop and linker tyrosines. Although we report here a similar autoactivation of both Abl and Arg through autophosphorylation, we do not observe autophosphorylation of the Abl activation loop even under the in vitro conditions used by Brasher and Van Etten. Moreover, we find that an Abl mutant containing a phenylalanine substitution at the activation loop tyrosine retains a normal ability to autoactivate. We conclude that autophosphorylation of Y412 does not contribute substantially to the Abl autoactivation we report here. Our results may differ from those of Brasher and Van Etten (4) because the enzymes were purified from different sources. It is possible, for example, that covalent modifications required for autophosphorylation of Y412 occur only during expression in mammalian cells.

In contrast to Abl, Arg has a modest ability to phosphorylate its activation loop tyrosine, and this activation loop phosphorylation contributes ~30% to Arg autoactivation. However, the Arg272F/439F mutant containing phenylalanine substitutions at both the linker and activation loop tyrosines retains the ability to autoactivate 3.7-fold. This indicates that autoactivation of Arg also requires phosphorylation of one or more sites in addition to the linker and activation loop tyrosines.

The protein domain encoded by the N-terminal exon of Abl was recently reported to form an inhibitory cap on the SH2 and kinase domains (26). We observe no difference in the basal kinase activities of Abl and Arg containing or lacking this cap. However, both Abl and Arg exhibit an enhanced ability to autoactivate when this N-terminal cap is removed. Release of the inhibitory cap from the SH2 and kinase domains may enhance autophosphorylation or may assist in formation of the activated confirmation induced by autophosphorylation. The reduced ability of capped Abl and Arg to autoactivate may explain why capped Abl exhibits reduced kinase activity upon expression in vivo (26).

Src family kinases may link diverse stimuli to activation of Abl family kinases. Abl family kinases are activated by a disparate collection of stimuli, including ionizing radiation, growth factor stimulation, adhesion receptor engagement, and oxidative stress (5, 11, 14, 18, 25, 30). Interestingly, Src family kinases are also activated by these stimuli (32), suggesting that Src family kinases may link these multiple stimuli to Abl and

Arg activation (Fig. 7B). Indeed, Src activity is required for Abl activation in response to platelet-derived growth factor (8, 25). We show here that the Src family kinase Hck directly activates both Abl and Arg through phosphorylation of their activation loops. Together, these results suggest that other Src family kinases may also activate Abl and Arg. It remains possible that Src family kinases differ in their abilities to activate Abl and Arg. These specificity differences could limit which Src family kinase signaling pathways interface with Abl and Arg.

How does the activation loop tyrosine become accessible for phosphorylation by Hck? The crystal structure of the nonphosphorylated Abl kinase domain (27) shows the activation loop tyrosine pointing into the interior of the kinase, making it inaccessible to phosphorylation when the kinase is in the inactive conformation. We find that nonactivated Abl and Arg are unable to efficiently phosphorylate their activation loop tyrosines in vitro, in accordance with the structural predictions and recent in vivo data (8). However, we find that Hck can phosphorylate Abl and Arg on their activation loops. It is unclear how the activation loop becomes available to Hck for phosphorylation. The binding of Hck to Abl or Arg may increase the structural plasticity of the activation loop or induce a conformational change that exposes Y412/Y439 for phosphorylation (23).

Increasing localized Abl or Arg concentration may facilitate autoactivation. Abl family kinases have been shown to autophosphorylate in *trans* (4, 8; A. L. Miller and A. J. Koleske, unpublished data). Thus, increasing their local concentration may facilitate kinase activation by autophosphorylation. Arg can bind cooperatively to F-actin (33), which may facilitate Arg clustering on actin filaments. This localized clustering of Arg might promote autoactivation. Oncogenic activation of Abl family kinases may also promote autoactivation. This is most commonly caused by a chromosomal translocation that fuses portions of the *bcr* gene to the *abl* gene. A coiled-coil oligomerization domain has been shown to be essential for the elevated tyrosine kinase activity of Bcr-Abl (20). In a similar fashion, the *tel* gene is fused to the *arg* gene in rare cases of acute myeloid leukemia (6, 12). The Tel fragment found in Tel-Arg has also been reported to dimerize, and Tel-Arg has elevated tyrosine kinase activity (6). Together, these observations strongly suggest that oligomerization of the kinases promotes kinase activation, but the exact mechanisms by which the Bcr and Tel moieties promote activation of their respective kinase fusion partners remain unclear. Multimerization of Abl and/or Arg might promote autophosphorylation in *trans*. Alternatively, a multimeric fusion protein might serve as a better substrate for activation by Src family kinases.

Activation loop phosphorylation leads to STI571 resistance. The Abl kinase domain has been shown to be resistant to STI571 upon phosphorylation of its activation loop (27). We demonstrate here that full-length Abl and Arg are both resistant to STI571 after phosphorylation of their activation loop tyrosines by Hck. Our observation suggests that Bcr-Abl may also become resistant to STI571 if it is phosphorylated on its activation loop. Some patients with chronic myelogenous leukemia in the blast crisis stage initially respond to STI571 but acquire resistance to treatment over time (9). Our data showing that Src family kinases render Abl resistant to STI571 suggest that upregulation of Src family kinases may contribute to STI571 resistance in chronic myelogenous leukemia patients.

Model for activation of Abl family kinases. We report here that two distinct phosphorylation pathways can activate Abl family kinases: (i) Abl and Arg can activate themselves through autophosphorylation of kinase domain tyrosines outside the activation loop and (ii) Src family kinases can activate Abl and Arg via phosphorylation of the activation loop tyrosine. We propose that the autophosphorylation pathway may allow Abl and Arg to integrate or amplify activating signals in a manner dependent on their own localized concentrations. For example, when local Abl concentrations are low, a Src family kinase would activate Abl through phosphorylation of the activation loop, leading to modest activation of downstream pathways (Fig. 7A). We hypothesize that this outcome would change if Abl were clustered locally within a cellular microenvironment. Following activating phosphorylation of its activation loop by Src family kinases, Abl would activate nearby Abl molecules by phosphorylating additional tyrosines (Fig. 7B). The additive effects of both stimulatory pathways would lead to a more robust activation of downstream pathways. In this fashion, the autoactivation pathway could allow Abl and Arg to amplify their signaling and integrate signals from distinct cell surface receptors.

ACKNOWLEDGMENTS

We are grateful to Xianyun Ye for technical assistance, Alex Zougman for mass spectrometric analyses, and the members of the Koleske laboratory and the three anonymous reviewers for helpful advice and comments on the manuscript.

This work was supported by NRSA grant MH67388 (K.Q.T.), USPHS grant NS39475 (A.J.K.), and a grant from the Edward J. Mallinckrodt, Jr., Foundation (A.J.K.).

REFERENCES

1. **Alexandropoulos, K., and D. Baltimore.** 1996. Coordinate activation of c-Src by SH3- and SH2-binding sites on a novel p130Cas-related protein, Sin. Genes Dev. **10:**1341–1355.
2. **Barila, D., and G. Superti-Furga.** 1998. An intramolecular SH3-domain interaction regulates c-Abl activity. Nat. Genet. **18:**280–282.
3. **Boyle, W. J., P. van der Geer, and T. Hunter.** 1991. Phosphopeptide mapping and phosphoamino acid analysis by two-dimensional separation on thin-layer cellulose plates. Methods Enzymol. **201:**110–149.
4. **Brasher, B. B., and R. A. Van Etten.** 2000. c-Abl has high intrinsic tyrosine kinase activity that is stimulated by mutation of the Src homology 3 domain and by autophosphorylation at two distinct regulatory tyrosines. J. Biol. Chem. **275:**35631–35637.
5. **Cao, C., X. Ren, S. Kharbanda, A. Koleske, K. V. Prasad, and D. Kufe.** 2001. The ARG tyrosine kinase interacts with Siva-1 in the apoptotic response to oxidative stress. J. Biol. Chem. **276:**11465–11468.
6. **Cazzaniga, G., S. Tosi, A. Aloisi, G. Giudici, M. Daniotti, P. Pioltelli, L. Kearney, and A. Biondi.** 1999. The tyrosine kinase abl-related gene ARG is fused to ETV6 in an AML-M4Eo patient with a t(1;12)(q25;p13): molecular cloning of both reciprocal transcripts. Blood **94:**4370–4373.
7. **Cooper, J. A., B. M. Sefton, and T. Hunter.** 1983. Detection and quantification of phosphotyrosine in proteins. Methods Enzymol. **99:**387–402.
8. **Dorey, K., J. R. Engen, J. Kretzschmar, M. Wilm, G. Neubauer, T. Schindler, and G. Superti-Furga.** 2001. Phosphorylation and structure-based functional studies reveal a positive and a negative role for the activation loop of the c-Abl tyrosine kinase. Oncogene **20:**8075–8084.
9. **Druker, B. J., C. L. Sawyers, H. Kantarjian, D. J. Resta, S. F. Reese, J. M. Ford, R. Capdeville, and M. Talpaz.** 2001. Activity of a specific inhibitor of the BCR-ABL tyrosine kinase in the blast crisis of chronic myeloid leukemia and acute lymphoblastic leukemia with the Philadelphia chromosome. N. Engl. J. Med. **344:**1038–1042.
10. **Franz, W. M., P. Berger, and J. Y. Wang.** 1989. Deletion of an N-terminal regulatory domain of the c-abl tyrosine kinase activates its oncogenic potential. EMBO J. **8:**137–147.
11. **Furstoss, O., K. Dorey, V. Simon, D. Barila, G. Superti-Furga, and S. Roche.** 2002. c-Abl is an effector of Src for growth factor-induced c-myc expression and DNA synthesis. EMBO J. **21:**514–524.

12. **Iijima, Y., T. Ito, T. Oikawa, M. Eguchi, M. Eguchi-Ishimae, N. Kamada, K. Kishi, S. Asano, Y. Sakaki, and Y. Sato.** 2000. A new ETV6/TEL partner gene, ARG (ABL-related gene or ABL2), identified in an AML-M3 cell line with a t(1;12)(q25;p13) translocation. Blood **95:**2126–2131.
13. **Jackson, P., and D. Baltimore.** 1989. N-terminal mutations activate the leukemogenic potential of the myristoylated form of c-abl. EMBO J. **8:**449–456.
14. **Kharbanda, S., R. Ren, P. Pandey, T. D. Shafman, S. M. Feller, R. R. Weichselbaum, and D. W. Kufe.** 1995. Activation of the c-Abl tyrosine kinase in the stress response to DNA-damaging agents. Nature **376:**785–788.
15. **Koleske, A. J., A. M. Gifford, M. L. Scott, M. Nee, R. T. Bronson, K. A. Miczek, and D. Baltimore.** 1998. Essential roles for the Abl and Arg tyrosine kinases in neurulation. Neuron **21:**1259–1272.
16. **Kraker, A. J., B. G. Hartl, A. M. Amar, M. R. Barvian, H. D. Showalter, and C. W. Moore.** 2000. Biochemical and cellular effects of c-Src kinase-selective pyrido[2,3-d]pyrimidine tyrosine kinase inhibitors. Biochem. Pharmacol. **60:**885–898.
17. **Kruh, G. D., R. Perego, T. Miki, and S. A. Aaronson.** 1990. The complete coding sequence of arg defines the Abelson subfamily of cytoplasmic tyrosine kinases. Proc. Natl. Acad. Sci. USA **87:**5802–5806.
18. **Lewis, J. M., R. Baskaran, S. Taagepera, M. A. Schwartz, and J. Y. Wang.** 1996. Integrin regulation of c-Abl tyrosine kinase activity and cytoplasmic-nuclear transport. Proc. Natl. Acad. Sci. USA **93:**15174–15179.
19. **Matsuda, M., B. J. Mayer, Y. Fukui, and H. Hanafusa.** 1990. Binding of transforming protein, P47gag-crk, to a broad range of phosphotyrosine-containing proteins. Science **248:**1537–1539.
20. **McWhirter, J. R., D. L. Galasso, and J. Y. Wang.** 1993. A coiled-coil oligomerization domain of Bcr is essential for the transforming function of Bcr-Abl oncoproteins. Mol. Cell. Biol. **13:**7587–7595.
21. **Miao, Y. J., and J. Y. Wang.** 1996. Binding of A/T-rich DNA by three high mobility group-like domains in c-Abl tyrosine kinase. J. Biol. Chem. **271:**22823–22830.
22. **Moarefi, I., M. LaFevre-Bernt, F. Sicheri, M. Huse, C. H. Lee, J. Kuriyan, and W. T. Miller.** 1997. Activation of the Src-family tyrosine kinase Hck by SH3 domain displacement. Nature **385:**650–653.
23. **Nagar, B., W. G. Bornmann, P. Pellicena, T. Schindler, D. R. Veach, W. T. Miller, B. Clarkson, and J. Kuriyan.** 2002. Crystal structures of the kinase domain of c-Abl in complex with the small molecule inhibitors PD173955 and imatinib (STI-571). Cancer Res. **62:**4236–4243.
24. **Piwnica-Worms, H., K. B. Saunders, T. M. Roberts, A. E. Smith, and S. H. Cheng.** 1987. Tyrosine phosphorylation regulates the biochemical and biological properties of pp60c-src. Cell **49:**75–82.
25. **Plattner, R., L. Kadlec, K. A. DeMali, A. Kazlauskas, and A. M. Pendergast.** 1999. c-Abl is activated by growth factors and Src family kinases and has a role in the cellular response to PDGF. Genes Dev. **13:**2400–2411.
26. **Pluk, H., K. Dorey, and G. Superti-Furga.** 2002. Autoinhibition of c-Abl. Cell **108:**247–259.
27. **Schindler, T., W. Bornmann, P. Pellicena, W. T. Miller, B. Clarkson, and J. Kuriyan.** 2000. Structural mechanism for STI-571 inhibition of abelson tyrosine kinase. Science **289:**1938–1942.
28. **Schindler, T., F. Sicheri, A. Pico, A. Gazit, A. Levitzki, and J. Kuriyan.** 1999. Crystal structure of Hck in complex with a Src family-selective tyrosine kinase inhibitor. Mol. Cell **3:**639–648.
29. **Sicheri, F., I. Moarefi, and J. Kuriyan.** 1997. Crystal structure of the Src family tyrosine kinase Hck. Nature **385:**602–609.
30. **Sun, X., P. Majumder, H. Shioya, F. Wu, S. Kumar, R. Weichselbaum, S. Kharbanda, and D. Kufe.** 2000. Activation of the cytoplasmic c-Abl tyrosine kinase by reactive oxygen species. J. Biol. Chem. **275:**17237–17240.
31. **Superti-Furga, G., S. Fumagalli, M. Koegl, S. A. Courtneidge, and G. Draetta.** 1993. Csk inhibition of c-Src activity requires both the SH2 and SH3 domains of Src. EMBO J. **12:**2625–2634.
32. **Thomas, S. M., and J. S. Brugge.** 1997. Cellular functions regulated by Src family kinases. Annu. Rev. Cell Dev. Biol. **13:**513–609.
33. **Wang, Y., A. L. Miller, M. S. Mooseker, and A. J. Koleske.** 2001. The Abl-related gene (Arg) nonreceptor tyrosine kinase uses two F-actin-binding domains to bundle F-actin. Proc. Natl. Acad. Sci. USA **98:**14865–14870.
34. **Wen, S. T., and R. A. Van Etten.** 1997. The PAG gene product, a stress-induced protein with antioxidant properties, is an Abl SH3-binding protein and a physiological inhibitor of c-Abl tyrosine kinase activity. Genes Dev. **11:**2456–2467.
35. **Xu, W., A. Doshi, M. Lei, M. J. Eck, and S. C. Harrison.** 1999. Crystal structures of c-Src reveal features of its autoinhibitory mechanism. Mol. Cell **3:**629–638.
36. **Xu, W., S. C. Harrison, and M. J. Eck.** 1997. Three-dimensional structure of the tyrosine kinase c-Src. Nature **385:**595–602.
37. **Yamaguchi, H., and W. A. Hendrickson.** 1996. Structural basis for activation of human lymphocyte kinase Lck upon tyrosine phosphorylation. Nature **384:**484–489.